

**SANDIA REPORT**

SAND84-2548 • Internal Distribution Only

Printed April 1985

# A Study of the Perforation of Widely Spaced Metal Plates

A. Keith Miller, Fred J. Zeigler

Prepared by  
Sandia National Laboratories  
Albuquerque, New Mexico 87185 and Livermore, California 94550  
for the United States Department of Energy  
under Contract DE-AC04-76DP00789

DEPARTMENT OF ENERGY DECLASSIFICATION REVIEW	
SINGLE REVIEW AUTHORIZED BY: <b>DOD 475.16</b>	DETERMINATION (CIRCLE NUMBER(S)): 1. CLASSIFICATION RETAINED 2. CLASSIFICATION CHANGED TO: 3. CONTAINS NO DOE CLASSIFIED INFO 4. COORDINATE WITH: 5. CLASSIFICATION CANCELLED 6. CLASSIFIED INFO BRACKETED 7. OTHER (SPECIFY): <i>Not reviewed</i>
REVIEWER NAME: <b>J.R. Schmidt</b>	
NAME: <b>B/13/08</b>	
DATE:	

Issued by Sandia National Laboratories, operated for the United States Department of Energy by Sandia Corporation.

**NOTICE:** This report was prepared as an account of work sponsored by an agency of the United States Government. Neither the United States Government nor any agency thereof, nor any of their employees, nor any of their contractors, subcontractors, or their employees, makes any warranty, express or implied, or assumes any legal liability or responsibility for the accuracy, completeness, or usefulness of any information, apparatus, product, or process disclosed, or represents that its use would not infringe privately owned rights. Reference herein to any specific commercial product, process, or service by trade name, trademark, manufacturer, or otherwise, does not necessarily constitute or imply its endorsement, recommendation, or favoring by the United States Government, any agency thereof or any of their contractors or subcontractors. The views and opinions expressed herein do not necessarily state or reflect those of the United States Government, any agency thereof or any of their contractors or subcontractors.

SAND84-2548  
Internal Distribution Only  
Printed April 1985

# **A Study of the Perforation of Widely Spaced Metal Plates**

A. Keith Miller  
Advanced Systems Division I  
Fred J. Zeigler  
Computational Physics and Mechanics Division I  
Sandia National Laboratories  
Albuquerque, NM 87185

## **Abstract**

The use of high-velocity metal rods to penetrate multiple, spaced plates of armor is being investigated for potential weapon systems applications. Two computational models were developed and a perforation test was performed to assess the initial performance of this concept as a basis for further development.

# Contents

Introduction .....	7
Ballistic Experiment .....	7
HULL Simulation of the Experiment .....	8
DRI Engineering Model Simulation of the Experiment.....	9
Experiment Results .....	10
Comparison of Simulations and Experiment .....	10
Recommendations for Future Work .....	11
References .....	11

## Figures

1 Ballistic Target Array .....	12
2 High-Velocity Oblique Impact Angle of Tungsten Penetrator .....	12
3 Sequential Density Plots After Penetration .....	13
4 Target Array Before Test .....	14
5 Front View of First Target Plate After Perforation by Tungsten Alloy Penetrator .....	15
6 Back View of First Target Plate After Perforation by Tungsten Alloy Penetrator .....	16
7 Sequential Views of Perforation of the First Plate .....	17
8 Front View of Second Target Plate After Test.....	21
9 Back View of Second Target Plate After Test .....	22
10 Front View of Third Target Plate After Test .....	23
11 Back View of Third Target Plate After Test .....	24
12 View of Deep Pits Formed in Front of Catcher Plate .....	25
13 Overall View of Target Array After Test.....	26

## Tables

1 HULL Computation Results for Impact of the First Plate .....	9
2 Perforation Parameters of DRI Model Simulation .....	10

# A Study of the Perforation of Widely Spaced Metal Plates

## Introduction

We are examining the feasibility of using small, high-velocity rods to penetrate multiple, widely spaced armor plates. To assess the performance of such weapon systems against a variety of target arrays and under differing impact conditions, a predictive model for the sequential perforation events is required. The parameters of interest in a perforation sequence are the residual mass of the penetrator as it exits each plate of the target array, as well as its residual velocity and tumble rate.

A semiempirical perforation model has been assembled by Mr. Rodney F. Recht and associates at the Denver Research Institute (DRI) in Denver, Colorado. Although the model is based on fundamental principles, several of the constants necessary to quantify the perforation must be determined from test data. These empirical constants have been published both for nondeforming penetrators impacting steel and aluminum plates and for penetrating materials that lose weight (erode), such as tungsten compounds and uranium alloys. This engineering model can predict all the perforation parameters of interest. However, because of its semiempirical basis and our lack of experience in using the model, a study was initiated to enhance our confidence in using the model for a variety of impact conditions and target arrays. The predictability of the tumble (yaw) characteristics of penetrators and tumbling rates is of particular interest since they seem to be the least well defined in the DRI model.

To increase confidence in the DRI model, we performed calculations using a three-dimensional finite difference hydrocode (HULL) and compared the results to the DRI model.<sup>1</sup> Although both sets of computations are based on certain assumptions and material descriptions, the types of assumptions made are different for the two calculations. A comparison of the two computational techniques appears to be a valid activity. A ballistic perforation experiment was performed to provide a benchmark for both sets of calculations.

Both models are necessary to understand the perforation of multiple, widely spaced plates. The DRI model permits rapid calculation of many perforation events, thus enabling a significant part of the design space to be evaluated quickly. However, when untested portions of the design space are evaluated, additional cross-checking is needed to assure that the model remains valid. For this reason the hydrodynamics code HULL was used to compute the perforation parameters for the more demanding impact events in order to gain insight into possible new phenomena that may not be implemented in the DRI code. For example, the hydrocode produces far more detailed information about the material flow field than does the engineering model.

This report describes the ballistic experiment that was conducted to provide a benchmark for the two models. Following the experiment description, results of the two computational efforts to model the experiment are presented. A brief discussion of the comparative results follows, along with recommendations for future test and computational activities.

## Ballistic Experiment

A target array of three target plates and a single backup (catcher plate) was assembled at the Sandia Live Fire Range (Figure 1). All three target plates were inclined so that the penetrator struck each at a 30° oblique angle. The first plate was rolled homogeneous armor (RHA), 4 in. thick; the second plate was HY-80 high-strength alloy steel, 2 in. thick; the third target plate was mild steel, 1 in. thick. The vertical backup plate was RHA, 5 in. thick.

An XM-839-E1 round designed for a 120-mm gun was launched at 5150 ft/s, using ~15 lb of propellant. The penetrator was a blunt-nosed Kennertium rod of ~90% tungsten powder with the remaining 10% a mixture of nickel, copper, and iron forming a matrix for the tungsten particles. This penetrator was 0.9 in.

in dia, 17.5 in. long (L/D ratio of 19), and weighed 9.3 lb. The penetrator's aluminum windshield and hardened, sharp steel point were removed to allow the blunted end of the penetrator to first contact the target plates.

The target array was positioned 300 ft from the gun to allow the sabot to be air-stripped before reaching the target. A series of vertical cardboard cards (yaw cards) were positioned at 10-ft intervals in front of the first plate of the target array to measure the attitude of the penetrator as it approached the target. The three cards closest to the target array contained conductive grids which, when broken by the penetrator, activated timing circuits to measure the velocity of the penetrator before impact with the first plate.

Six high-speed motion picture cameras and two image motion cameras were trained on the target, as shown in Figure 1, to obtain velocity data and to determine the attitude of the penetrator as it progressed through the target array. Although the test yielded good film records, excessive debris obscured the penetrator so no velocity data were obtained after impact with the first plate.

## HULL Simulation of the Experiment

The experiment described above was modeled with a HULL computation, restricted to the perforation of the first plate. Fins were not included as part of the penetrator, which was modeled as a cylinder.

Figure 2 shows the oblique impact angle between the penetrator and target just before impact. The section shown lies in the x-z plane with the y-axis coming vertically out of the page (so that  $y = 0$  in the figure).

A three-dimensional computation of the problem was done on a  $36 \times 18 \times 128$  x-y-z grid. From the initial setup of Figure 2 the calculation was run in the reverse ballistic mode, with the plate moving toward the stationary penetrator at 5300 fps (the intended experimental velocity of the penetrator).

The HULL hydrocode produces approximate solutions to the partial differential equations of continuum mechanics. These equations represent the conservation of mass, momentum, and energy for each of the materials in the problem. Additionally, equations of state, along with certain material properties,

must be implemented for each material to determine the stress as a function of the strain. In HULL, viscous effects are not included in the physics.

The equations of motion are solved in finite difference form. Thus, the differential equations discussed above, which are valid for all points in space, are replaced by a set of algebraic finite difference equations, valid at the grid points. Given the values of the density, energy, velocities, and stress for each material at each grid point at a certain time, the problem is then advanced to the next time value by solving the finite difference equations.

The penetrator was modeled as pure tungsten, with a yield strength of 290 000 psi and a density of 0.65 lb/in<sup>3</sup>. For RHA we assumed a yield strength of 217 500 psi with a density of 0.28 lb/in<sup>3</sup>.

A useful relationship that determines the strain field in the impacting materials is the relationship between the shock speed in the material, the particle speed, and the sound (elastic strain wave) speed. This relationship is  $U_s = C_o + S U_p$ , where  $U_s$  is the shock wave speed,  $C_o$  is the sonic velocity, and  $U_p$  is the particle velocity. The instantaneous particle velocity is a function of the pressure field. The sound speed and the empirically determined constant,  $S$ , are considered material parameters. For tungsten,  $C_o = 1.57 \times 10^5$  in./s,  $S = 1.27$ . For the RHA,  $C_o = 1.82 \times 10^5$  in./s,  $S = 1.73$ .

To compute the yaw rate after perforation, it was necessary to compute the angular momentum of the remaining part of the penetrator. Cells that contained tungsten that was separated from the main mass of the penetrator were discarded. The angular momentum of the tungsten in the remaining cells around the center of mass was computed, then summed over all the cells to get the final result. The moment of inertia was computed in a similar way, then these two numbers were used to compute the angular velocity (yaw rate).

Density plots of various stages of the calculation are presented in Figure 3, views (a) through (d). The contours shown are curves of constant density, with values of the density ranging from 0.09 to 0.62 lb/in<sup>3</sup>. The curves indicate the outlines of the different material shapes in the configuration. As shown in the plots, the diameter of the hole is about 2-2/3 times as large as the original diameter of the penetrator.

A few results are summarized in Table 1. The quantities given refer to the penetrator.

**Table 1. HULL Computation Results for Impact of the First Plate**

	Initial	Exiting First Plate
Velocity (fps)	5300	4550
Weight (lb)	5.764	5.104
Length (in.)	17.75	11
Yaw rate (°/s)	0	5000*

\*Toward the normal axis of the plate

For further information about the HULL code, see Reference 1.

## DRI Engineering Model Simulation of the Experiment

The engineering model formulated at the Denver Research Institute can be used to calculate the residual mass, velocity, and attitude of a penetrator as it passes through a series of target plates. This model was exercised to simulate the ballistic test described in Experiment Results.

The features of the DRI model are described in References 2 through 4. A comparison of this model to other ballistic impact models has been performed,<sup>5</sup> which indicates that this model is probably the most conservative of the models available to date. The comparative results presented show that the method of calculating the ballistic limit velocity and the residual velocity in the DRI model is similar to other methods, although the DRI model adds some empirically derived constants to adjust those values for penetrators that lose mass and change shape.<sup>4</sup> The method of calculating the mass loss is unique in the DRI model in that it first calculates the mass loss due to erosion while the interface-relative velocity between the target plate and the penetrator is greater than the plastic wave speed in the penetrator. The

model then calculates the additional mass loss of the penetrator caused by extrusion of the nose and subsequent shear of the extrusion lips. This is followed by a calculation to determine whether damaging bending moments are applied to the penetrator for sufficient time to cause the penetrator to break up or shatter.

An empirical relationship predicting the tumble rate of the penetrator as it exits each plate, based on the penetrator impact attitude, length, velocity, and plate thickness, is included in the model.

The pertinent material properties for the target plates are shown in Figure 1. A density of 0.28 lb/in<sup>3</sup> was assigned to each of the plates. The properties assigned to the tungsten alloy penetrator are as follows:

Density	0.63 lb/in <sup>3</sup>
Brinell hardness number	295
Compressive modulus	$5.30 \times 10^7$ psi
Static yield strength	$1.27 \times 10^5$ psi
Dynamic yield strength	$1.68 \times 10^5$ psi
Strain to failure	0.29
Percentage reduction of area	23%
Plastic wave velocity	100 in./s

The desired initial impact velocity of 5300 fps was not achieved in the test (5150 fps was obtained). However, because no residual velocity information was obtained, the two computational simulations (the HULL model and the DRI model) were not rerun at the actual test impact velocity. The desired impact velocity of 5300 fps was used in both the HULL and DRI models so that the two computations could be compared.

The perforation parameters calculated by the DRI model simulation of the test are shown in Table 2. Note that the initial length, diameter, and weight of the penetrator used in the HULL and DRI model calculations are slightly different than for the penetrator used in the experiment. The calculations were performed before the experiment, using estimates of the penetrator geometry. Since considerable computer time is needed to perform the HULL calculations, and because insufficient information was obtained from the experiment to benchmark the calculations, the same penetrator geometry was used in both sets of calculations, and the HULL calculations were not repeated.

**Table 2. Perforation Parameters of DRI Model Simulation**

	Initial	Exit First Plate	Exit Second Plate	Exit Third Plate
Velocity (fps)	5300	4688	4182	3818
Weight (lb)	5.80	3.21	2.22	1.76
Length (in.)	17.75	9.83	6.80	5.37
Yaw rate (°/s)*	0	6140	10 125	3257

\*The direction of tumble is assumed to be random in these calculations. The actual attitude of the penetrator on subsequent impacts is the RMS value of the initial attitude and the calculated change to the next plate.

## Experiment Results

The ballistic experiment yielded mixed results. The mechanics of the experiment went well; the penetrator was launched to nearly the desired velocity, the timing sequence for the high-speed photography operated successfully, and the perforation of each plate was observed. However, the primary objectives of the test, which were to determine the residual velocity, mass, and attitude of the penetrator as it exited each plate, were not achieved because of the excessive debris and fire generated by the perforation.

Figure 4 is a photograph of the target array before the test. Figures 5 and 6 are photographs of the front and back, respectively, of the first target plate after it was perforated by the tungsten alloy penetrator. The 0.9-in.-dia penetrator created a clean hole, ~2.5 in. in dia, completely through the plate. Figure 7, views (a) through (g), is a sequence of stop-motion photographs taken from a quadrasplit-shutter, high-speed camera (~20 000 frames per second) of the perforation of the first plate. The extremely bright flash at the end of this sequence was caused when the aluminum-stabilizing fin vaporized on impact with the steel plate.

Figures 8 and 9 are photographs of the front and back, respectively, of the second target plate after the test. Two major holes were formed near the base of the plate. The penetrator trajectory was expected to deviate upward, toward the normal of the first plate, so a low aim point was chosen on the first plate. The penetrator did not deviate upward appreciably from its initial trajectory and struck the cross brace near the bottom of the second target plate. We speculate that impact broke the penetrator into two pieces. One piece formed a glancing penetration at the bottom of

the plate, and the other a clean hole nearly 1.5 in. in dia about 1 ft from the bottom of the plate.

Figures 10 and 11 are photographs of the front and back, respectively, of the third target plate after the test. Six complete perforations and one nearly complete perforation were found in this 1-in.-thick plate. The plate was also deeply pitted.

Figure 12 shows the deep pits formed in the front of the very thick, vertical catcher plate.

Figure 13 shows the overall condition of the target array following the test.

Although it is likely that the penetrator had a high tumble rate after impact with the cross brace at the base of the second target plate, it still successfully penetrated the remainder of the target array. The amount of debris damage to the target plates was probably greater than was initially expected, even though the sizes of the debris fragments were small.

## Comparison of Simulations and Experiment

Because the residual mass, velocity, and attitude data were not obtained from the experiment, most of the comparative information is based on the HULL and DRI model simulations.

The DRI simulation predicted that the penetrator would perforate all three target plates; this was accomplished in the experiment. The simulation also predicted that about 30% of the penetrator weight would impact the vertical catcher plate. However, from the number of holes in the third target plate and the depth of the craters in the vertical catcher plate, it does not appear that 30% of the penetrator reached the catcher plate. The unfortunate impact of the penetrator with the horizontal cross brace at the second target plate probably broke it into two pieces and caused high rates of tumbling in those two pieces, which increased their fragmentation. Those effects were not anticipated in the DRI simulation.

Reasonably good agreement was demonstrated between the two computational simulations, although slightly different penetrator material properties were used. The agreement in the prediction of the residual velocity was especially good, less than 3% difference. The residual lengths predicted are also in good agreement, although the residual weights are at some variance.

The HULL simulation predicted the residual weight of the penetrator to be 88.5% of the initial weight; the DRI simulation predicted the residual weight to be only 55% of the initial weight. This

variance is a result of the different methods used to model the perforation events. The DRI model allows only a short distance of the penetrator to extrude to a larger diameter, which is then sheared off by the target plate to a diameter 1.25 times the original penetrator diameter. The rest of the penetrator remains at its original diameter. The HULL model does not incorporate such an arbitrary material loss mechanism and, as can be seen in the density plots of the HULL results, the penetrator extrudes to a larger diameter throughout a large percentage of its length. This accounts for the agreement in length but disagreement in weight.

One of the major reasons for performing the HULL calculations was to check the empirical relationship for the penetrator tumble rate that was used in the DRI model. The agreement in the tumble rates was surprisingly good. The HULL simulation predicted a tumble rate of  $5000^\circ/\text{s}$ , whereas the DRI model predicted  $6140^\circ/\text{s}$ .

The diameter of the hole pierced through the first plate ( $\approx 2.5$  in.) was very close to the diameter predictions made in the HULL computations. This indicates that the material displacement process (the pressure and velocity fields) simulated in the HULL computations are in good agreement with the actual process in the perforation event.

## Recommendations for Future Work

The major portion of future work should be directed toward obtaining adequate experimental data to benchmark the HULL and DRI simulations. Special emphasis should be placed on obtaining data on the size, attitude, and velocity of the penetrating rod immediately after it exits each plate of the target array. Flash x-ray equipment will provide images of

the main portion of the ballistic penetrators. However, highly accurate timing information is required with the x-ray images to determine the parameters of interest.

We need to develop statistics by repeatedly testing a particular target array at a given set of impact conditions. Several extremes of the possible design space also need to be tested and analyzed by computational simulations. The effects of material models and properties (state equations) on the perforation performance need to be explored in the simulations.

We also need to develop better methods for measuring the damage potential of the dense debris cloud in the ballistic experiments.

In sum, the combined efforts of simulating ballistic experiments and the actual performance of such experiments are necessary to understand, and later to optimize, the perforation of multiple plate target arrays.

## References

- <sup>1</sup>D. A. Matuska, *HULL Users Manual*, AFATL-TR-84-59, June 1984.
- <sup>2</sup>Rodney F. Recht and Jerome D. Yatteau, "Multiple Plate Penetration Modeling for Deforming and Yawing Ballistic Penetrators Which Lose Mass," *Seventh International Symposium on Ballistics Proceedings*, The Hague, The Netherlands, 19-21 April 1983, pp 271-80.
- <sup>3</sup>Rodney F. Recht, "Taylor Ballistic Impact Modelling Applied to Deformation and Mass Loss Determinations," *Int J of Eng Sci*, 16:809-27 (1978).
- <sup>4</sup>Rodney F. Recht, "Rod Penetration and Component Vulnerability Modeling," private communication with A. K. Miller, Division 1651, Sandia National Laboratories, Albuquerque, NM, 6 September 1983.
- <sup>5</sup>A. Keith Miller, *An Evaluation of Three Engineering Models for Predicting the Ballistic Perforation of Multiple Plates by Long Rods*, SAND83-2246 (Albuquerque, NM: Sandia National Laboratories, March 1983).

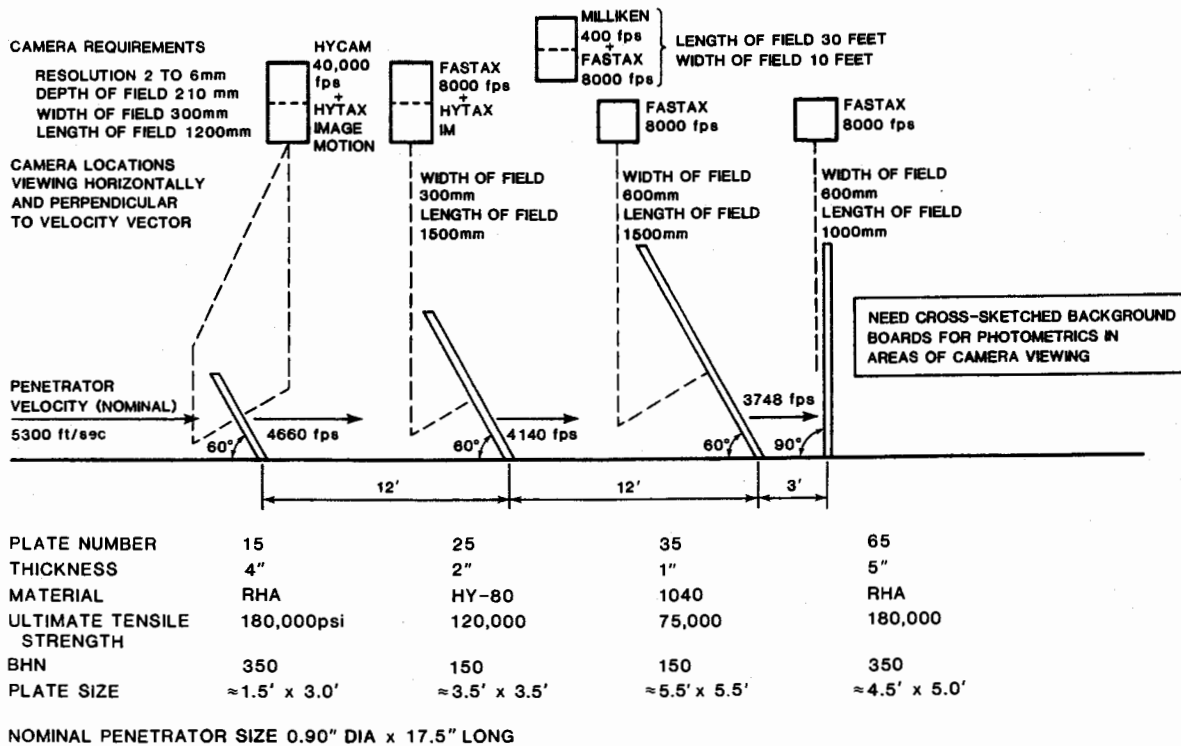


Figure 1. Ballistic Target Array

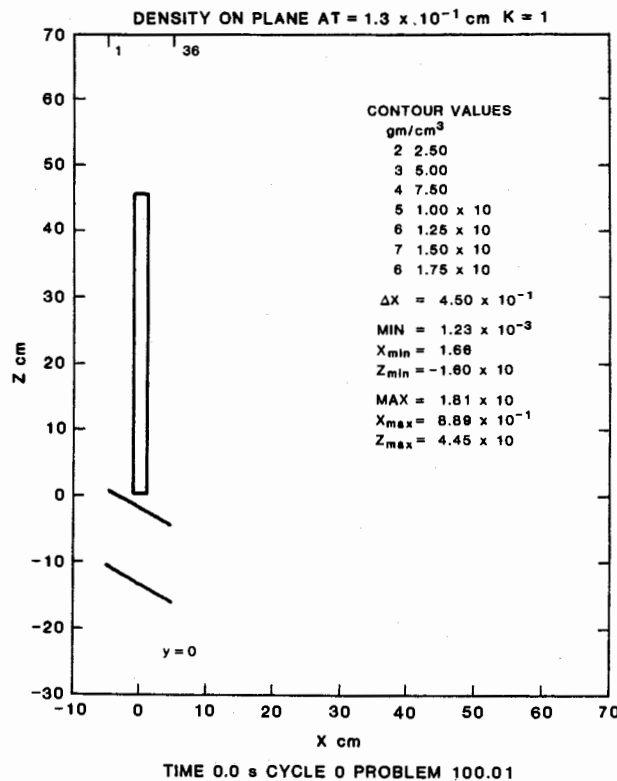
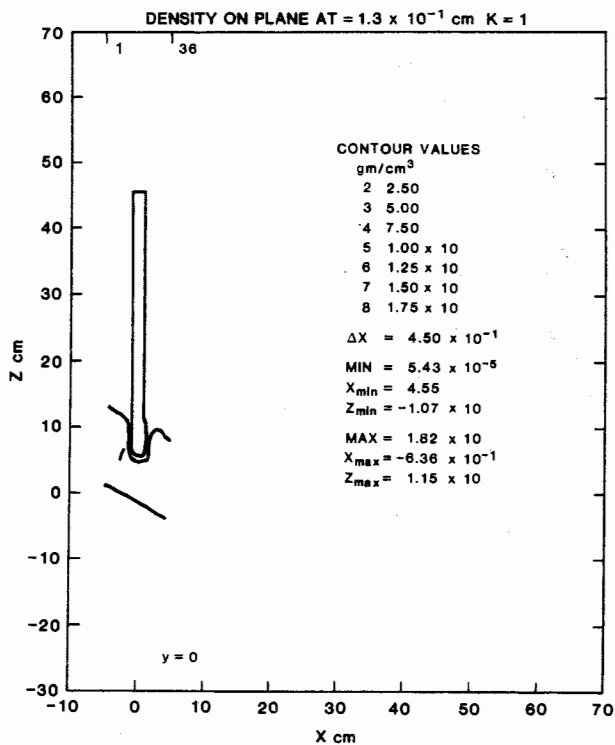
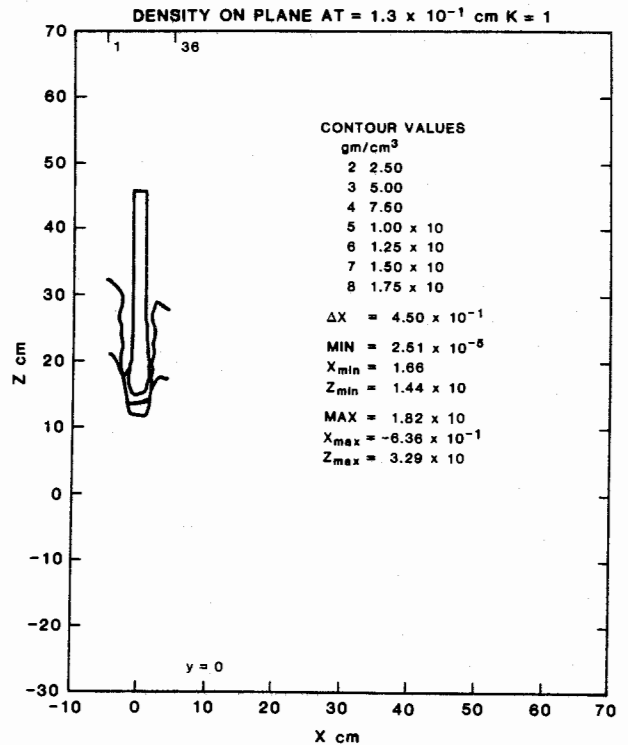


Figure 2. High-Velocity Oblique Impact Angle of Tungsten Penetrator



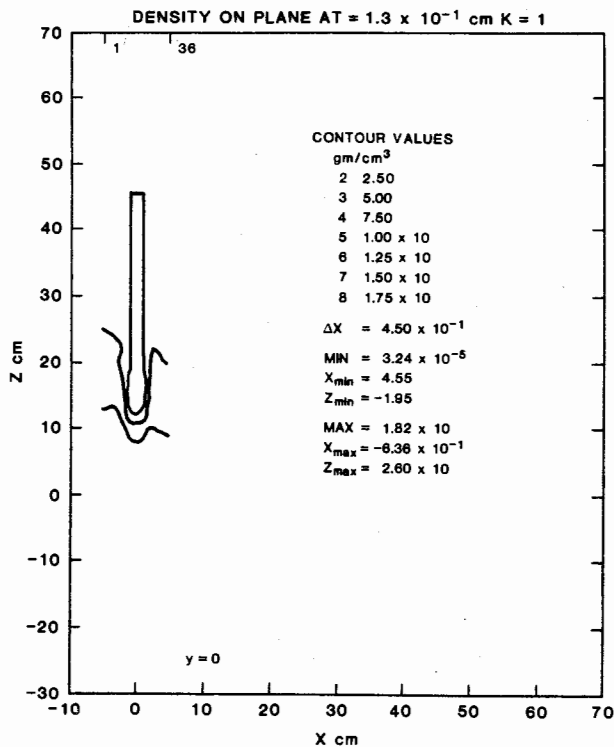
TIME 75.000  $\mu$ s CYCLE 263 PROBLEM 100.0

View (a)



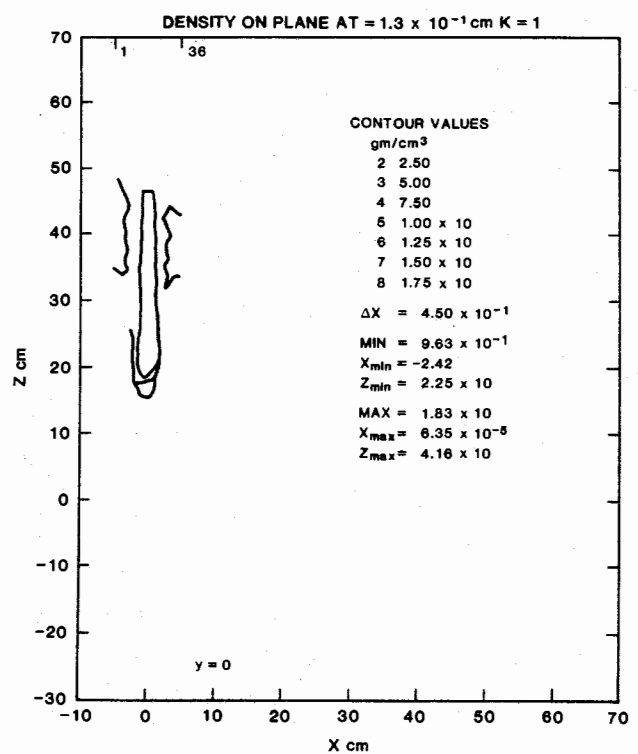
TIME 200.000  $\mu$ s CYCLE 696 PROBLEM 100.01

View (c)



TIME 152.507  $\mu$ s CYCLE 531 PROBLEM 100.0

View (b)



TIME 300.000  $\mu$ s CYCLE 1041 PROBLEM 100.01

View (d)

Figure 3. Sequential Density Plots After Penetration

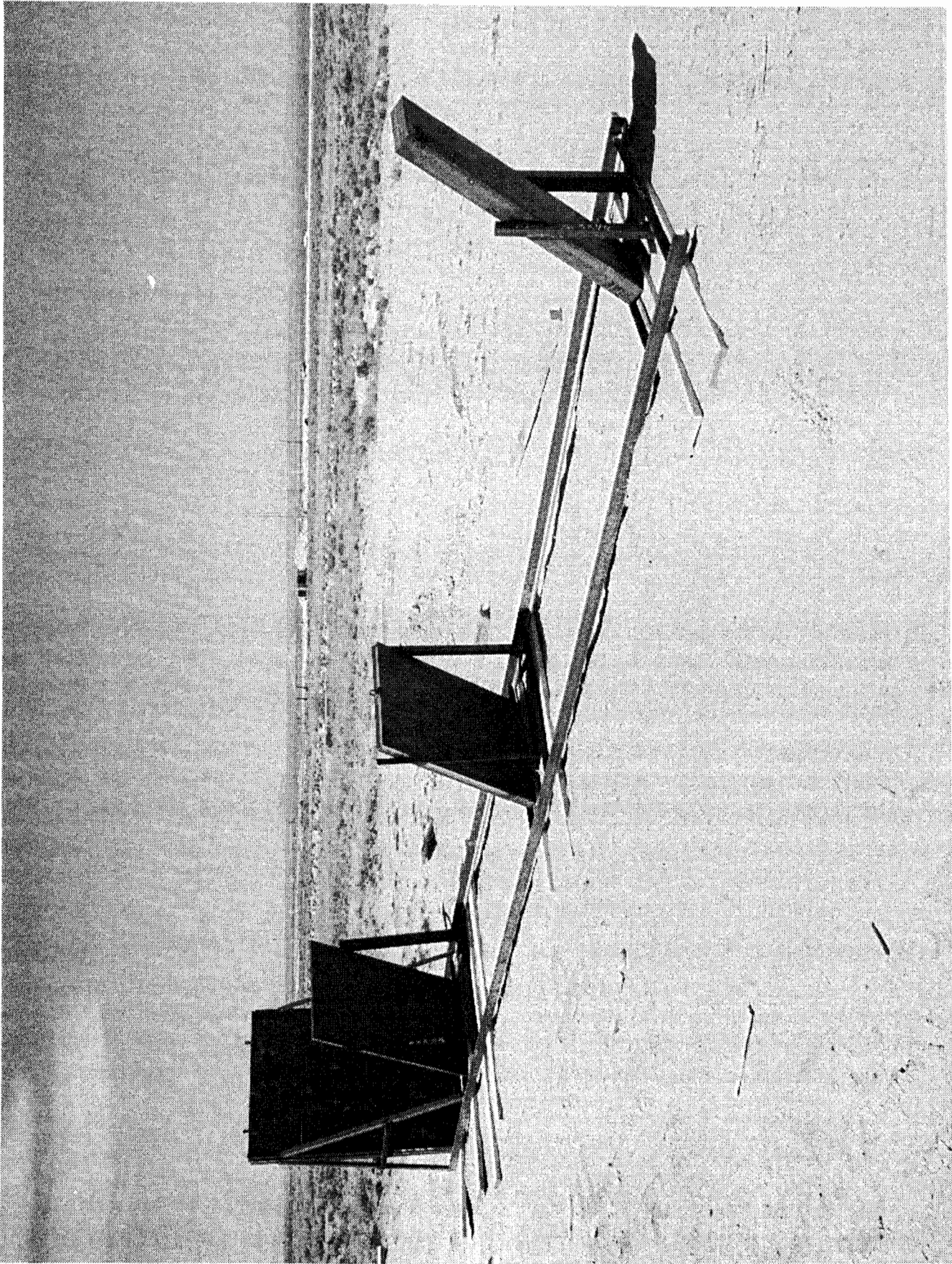


Figure 4. Target Array Before Test

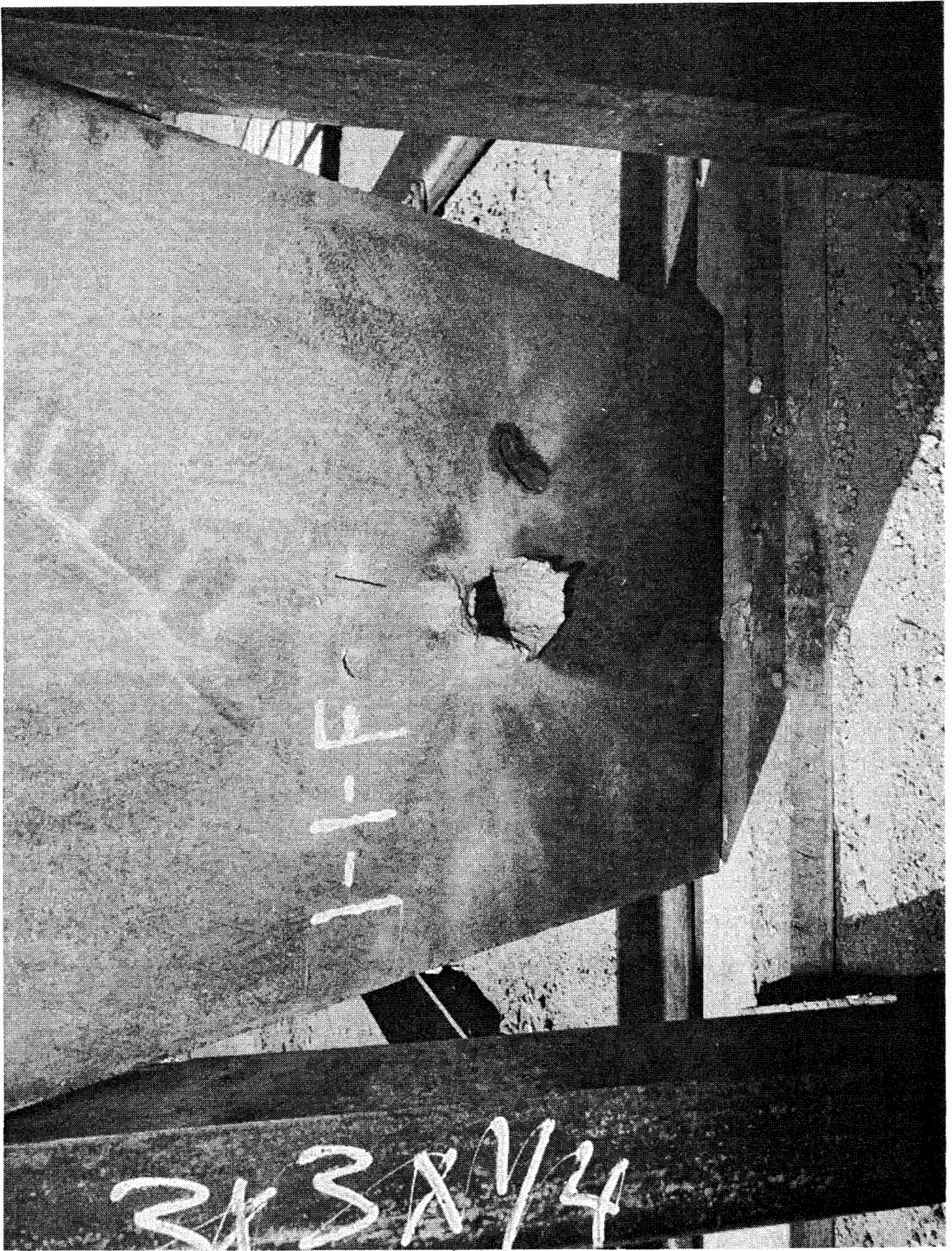


Figure 5. Front View of First Target Plate After Perforation by Tungsten Alloy Penetrator

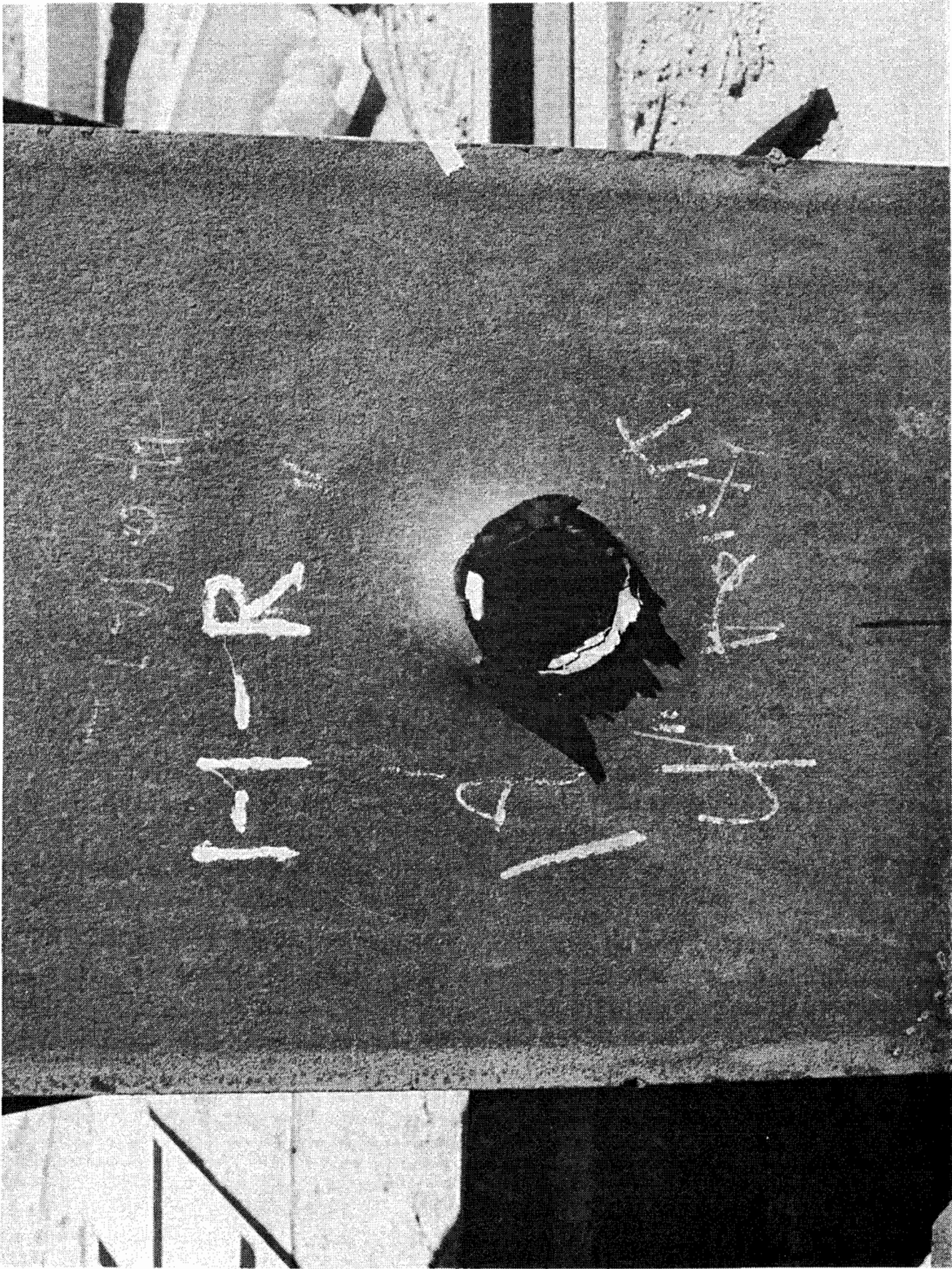
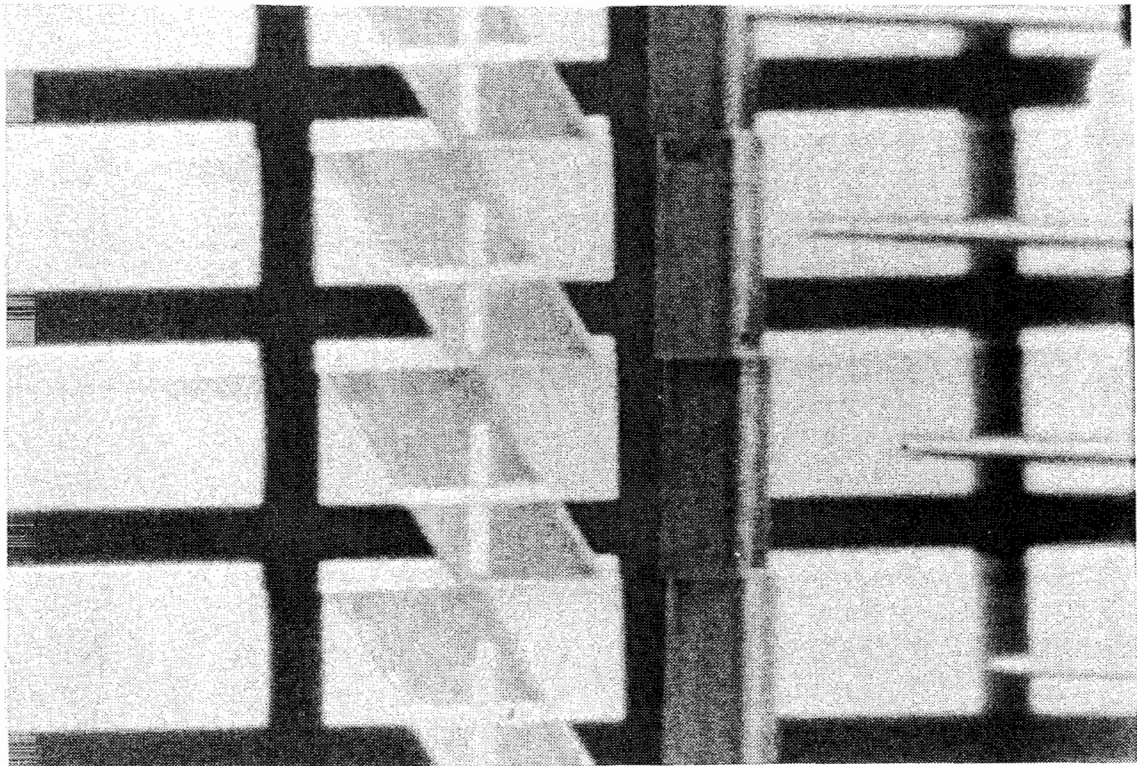
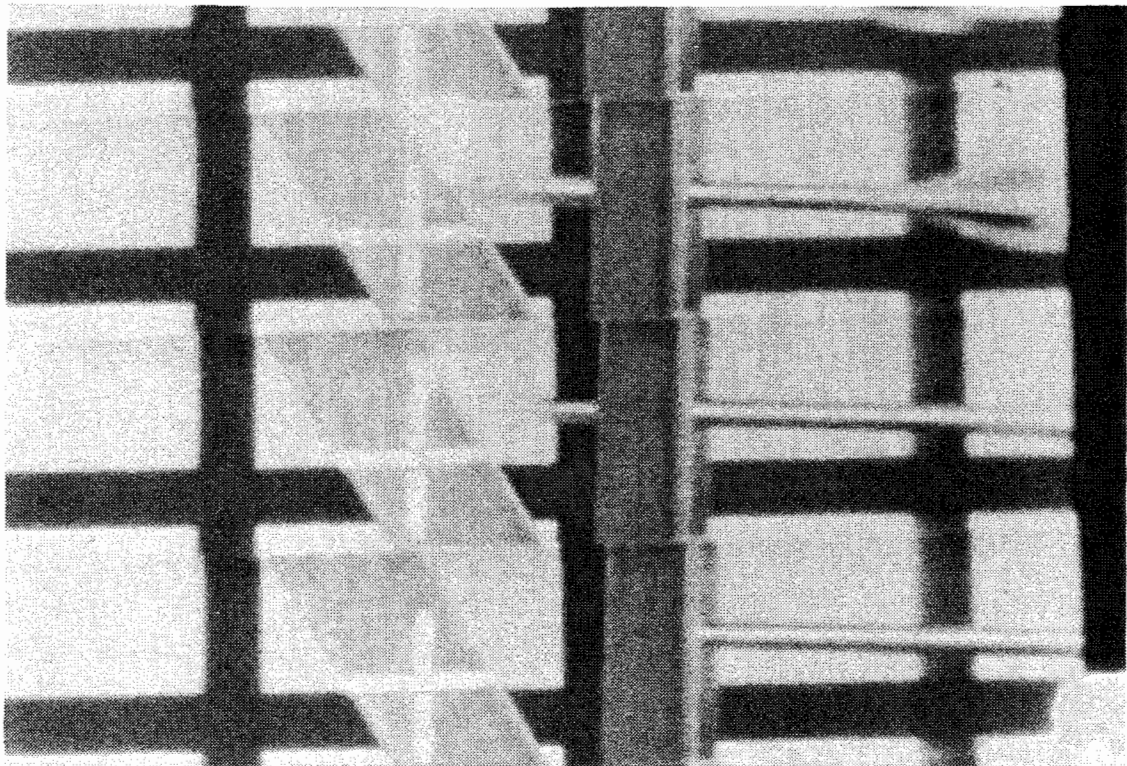


Figure 6. Back View of First Target Plate After Perforation by Tungsten Alloy Penetrator

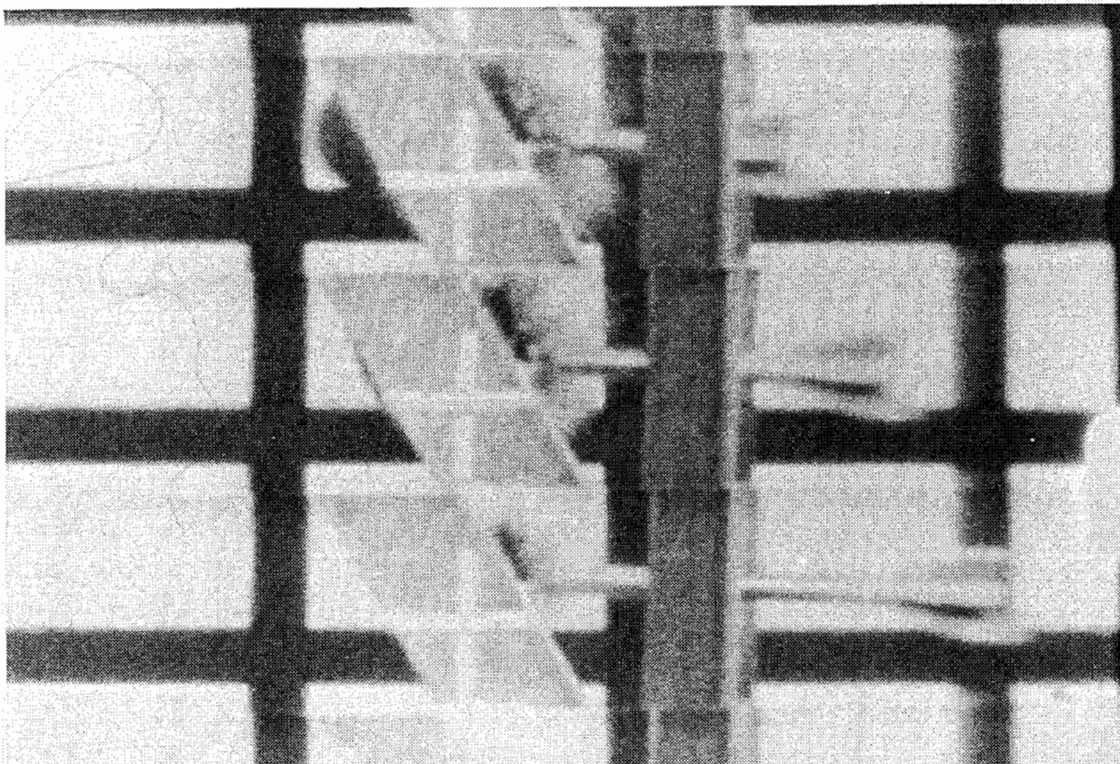


View (a)

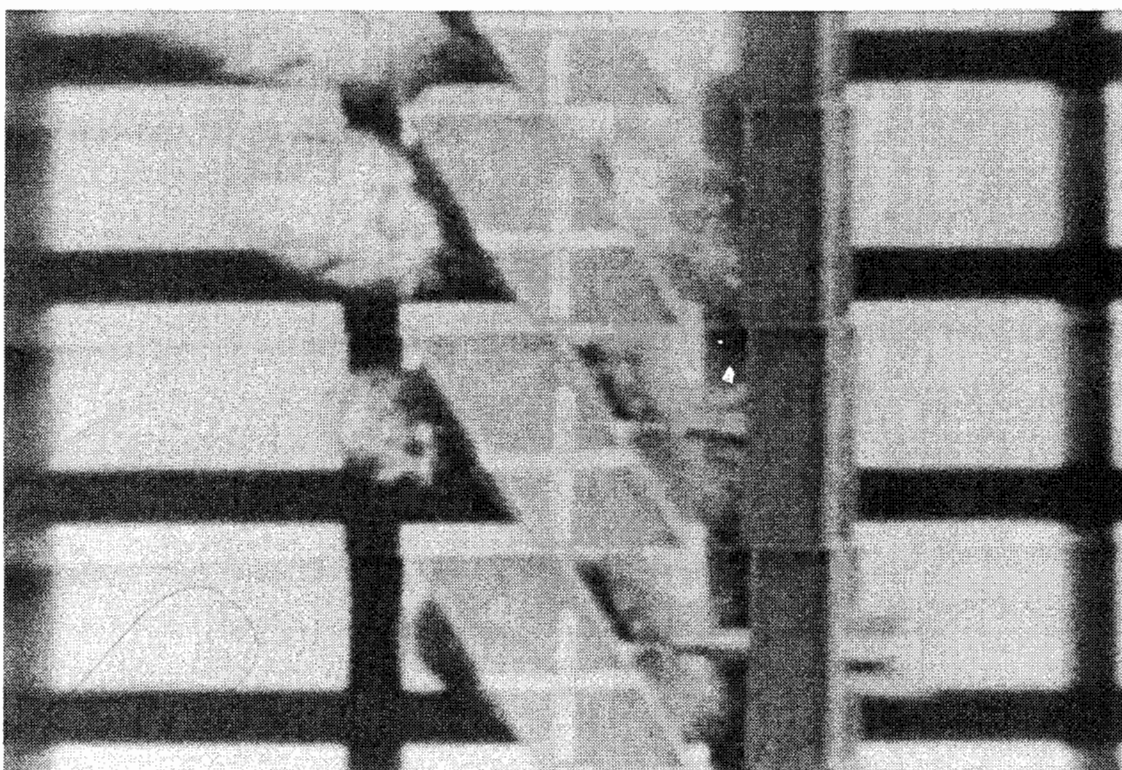


View (b)

**Figure 7.** Sequential Views of Perforation of the First Plate

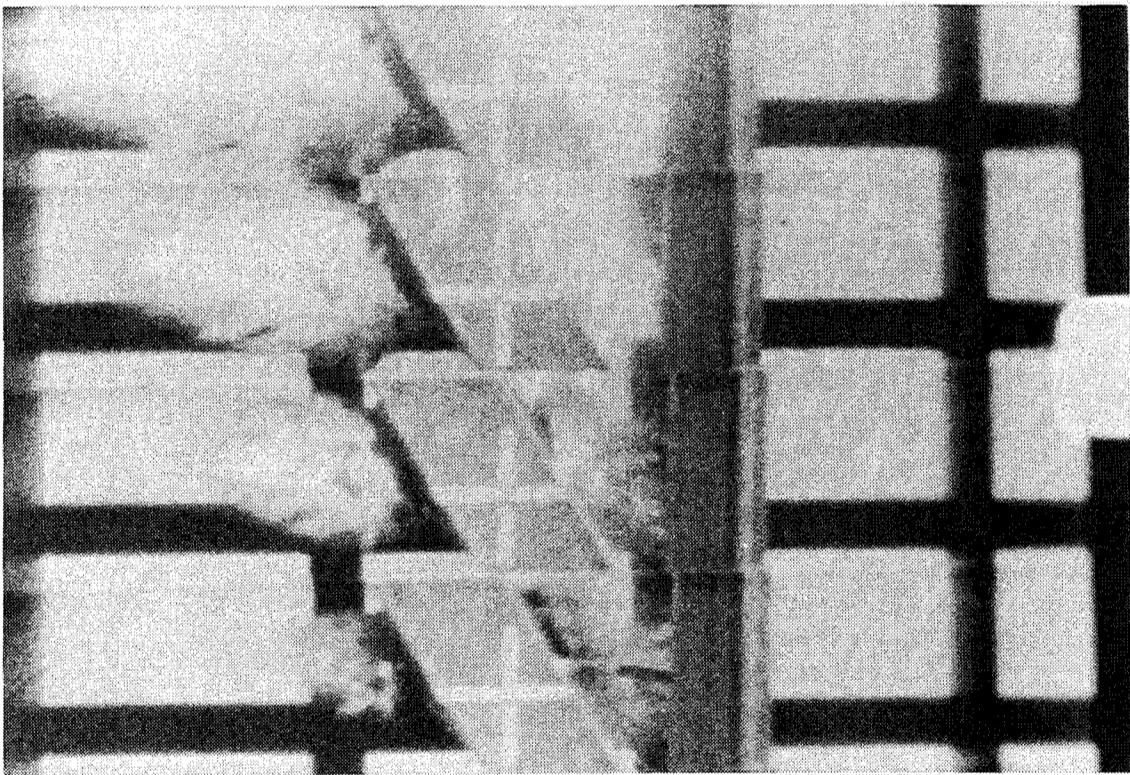


View (c)

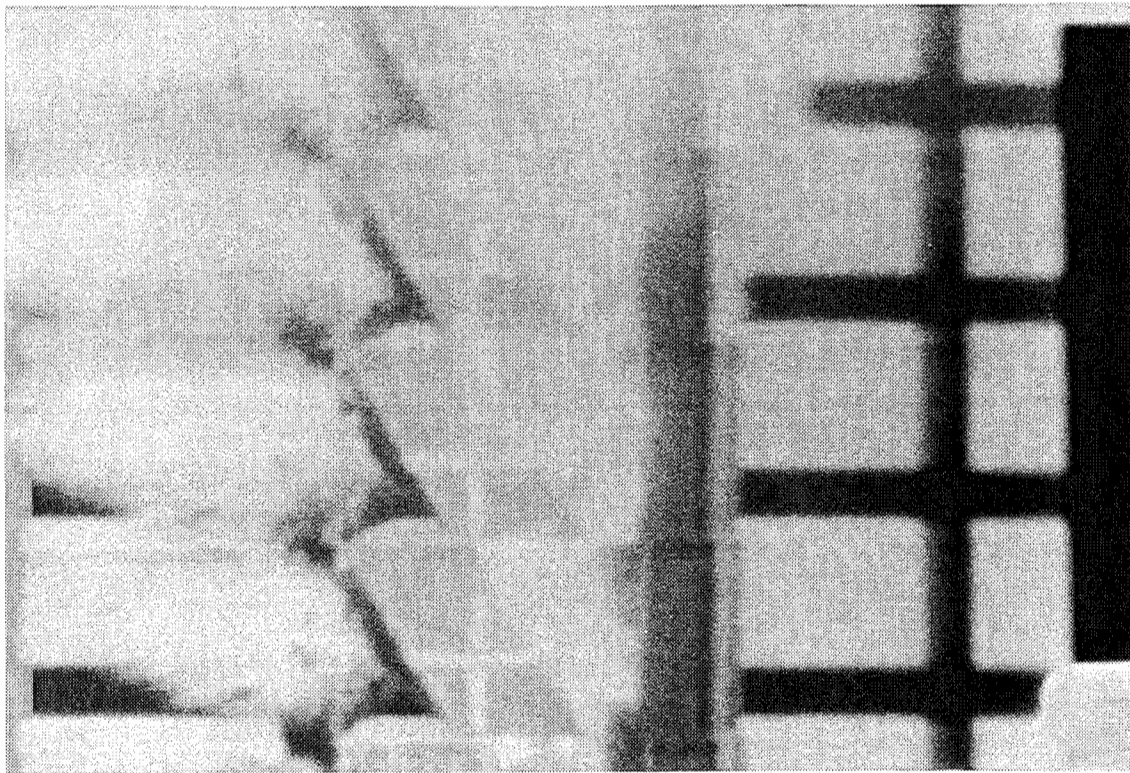


View (d)

**Figure 7.** (Continued)

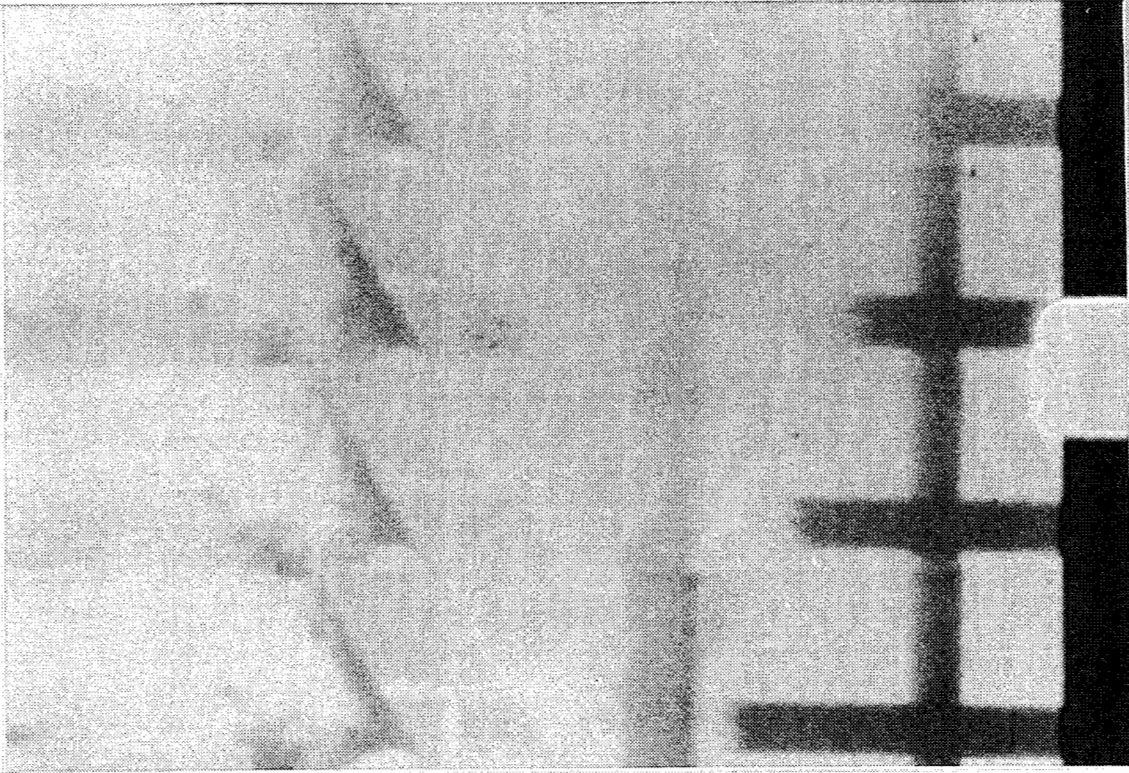


View (e)



View (f)

**Figure 7.** (Continued)



View (g)

**Figure 7.** (Concluded)

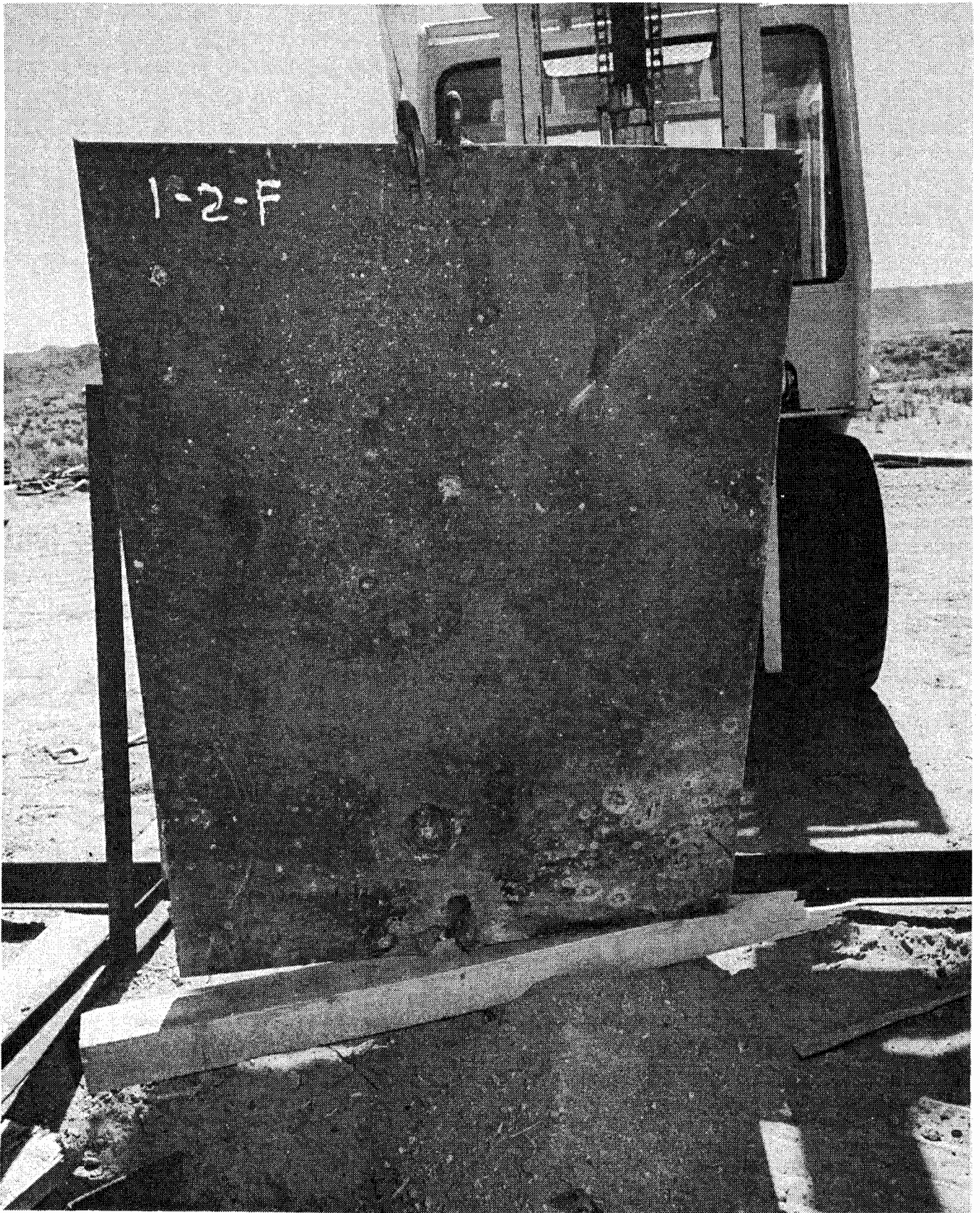


Figure 8. Front View of Second Target Plate After Test

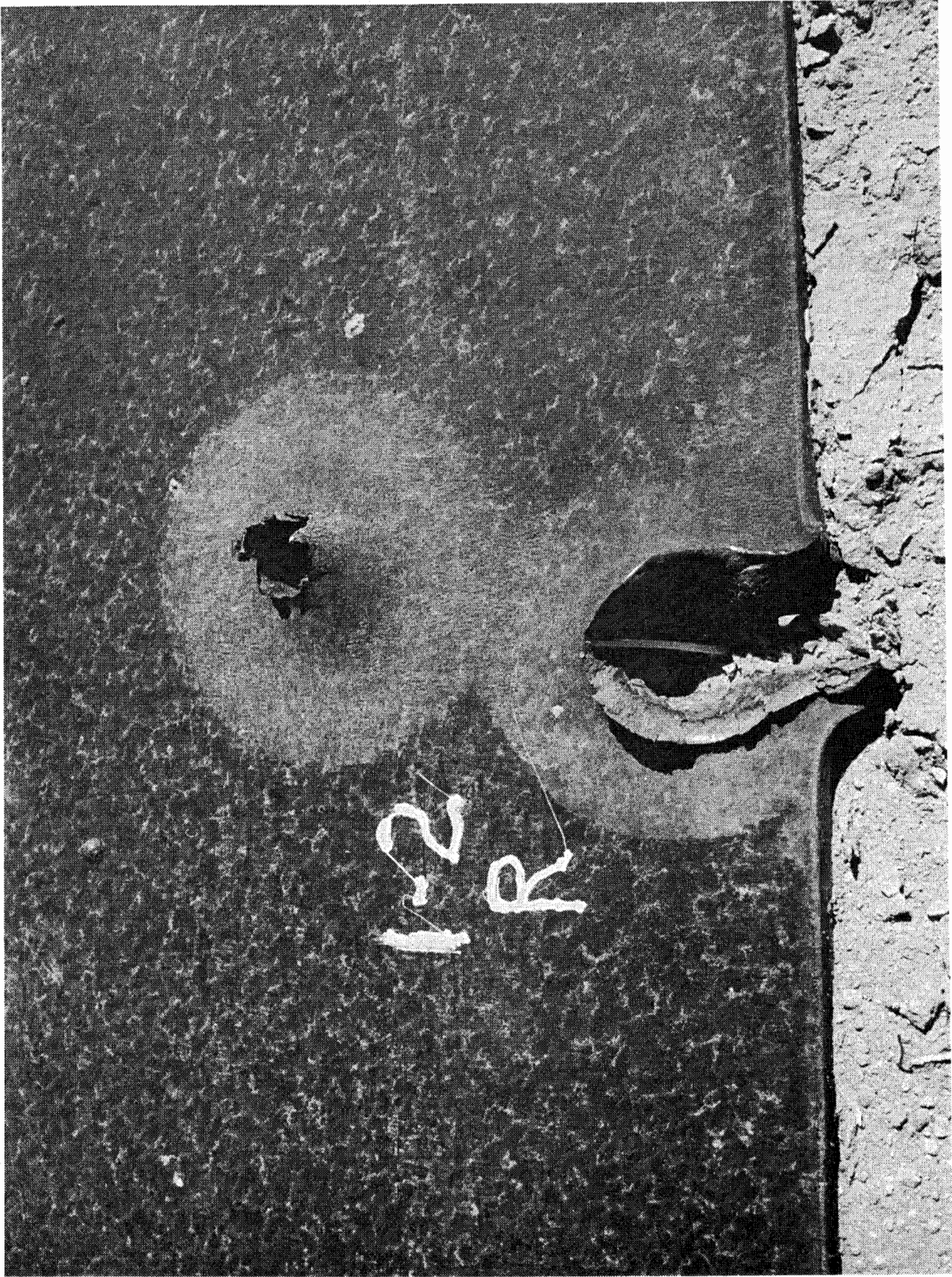


Figure 9. Back View of Second Target Plate After Test

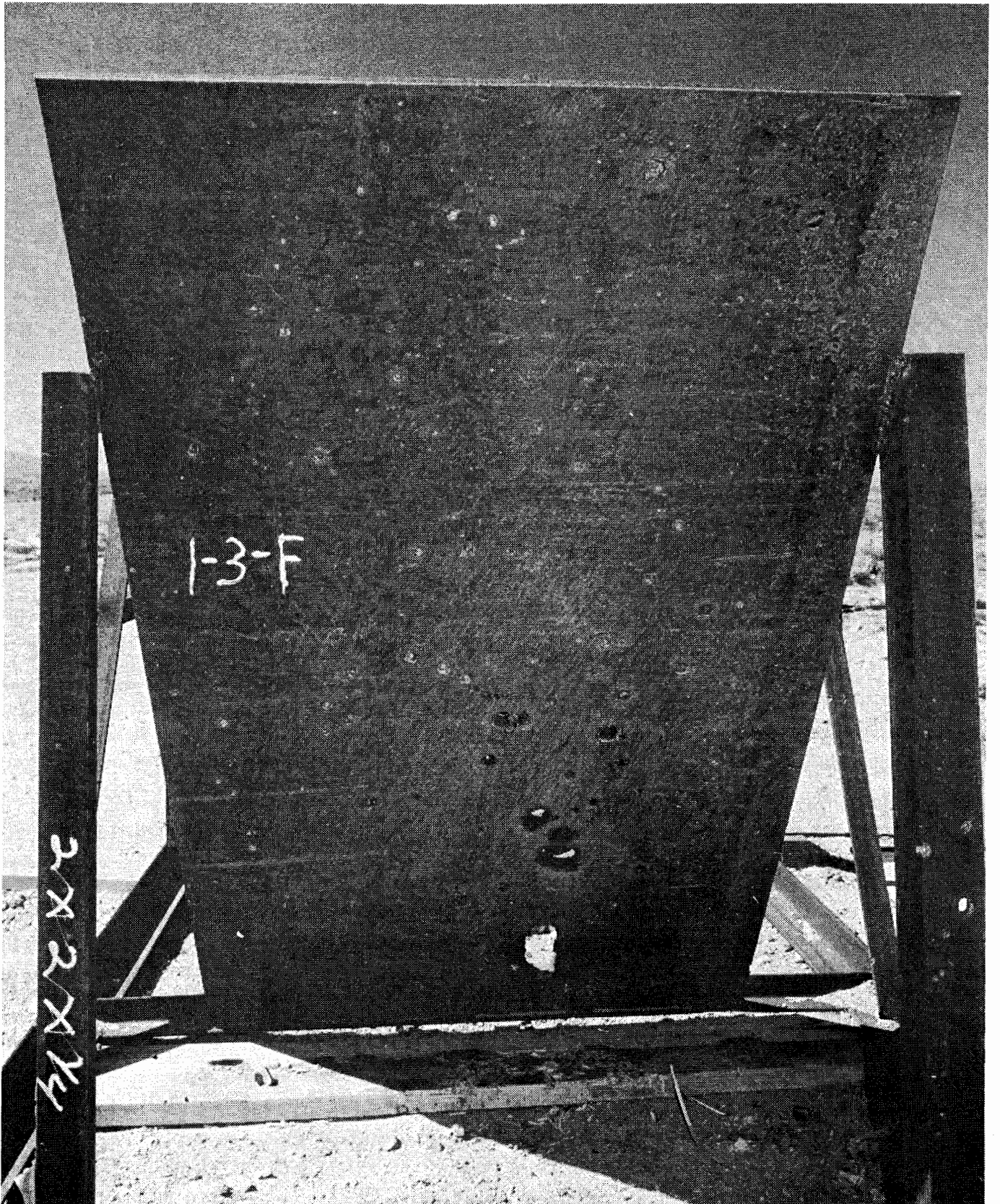
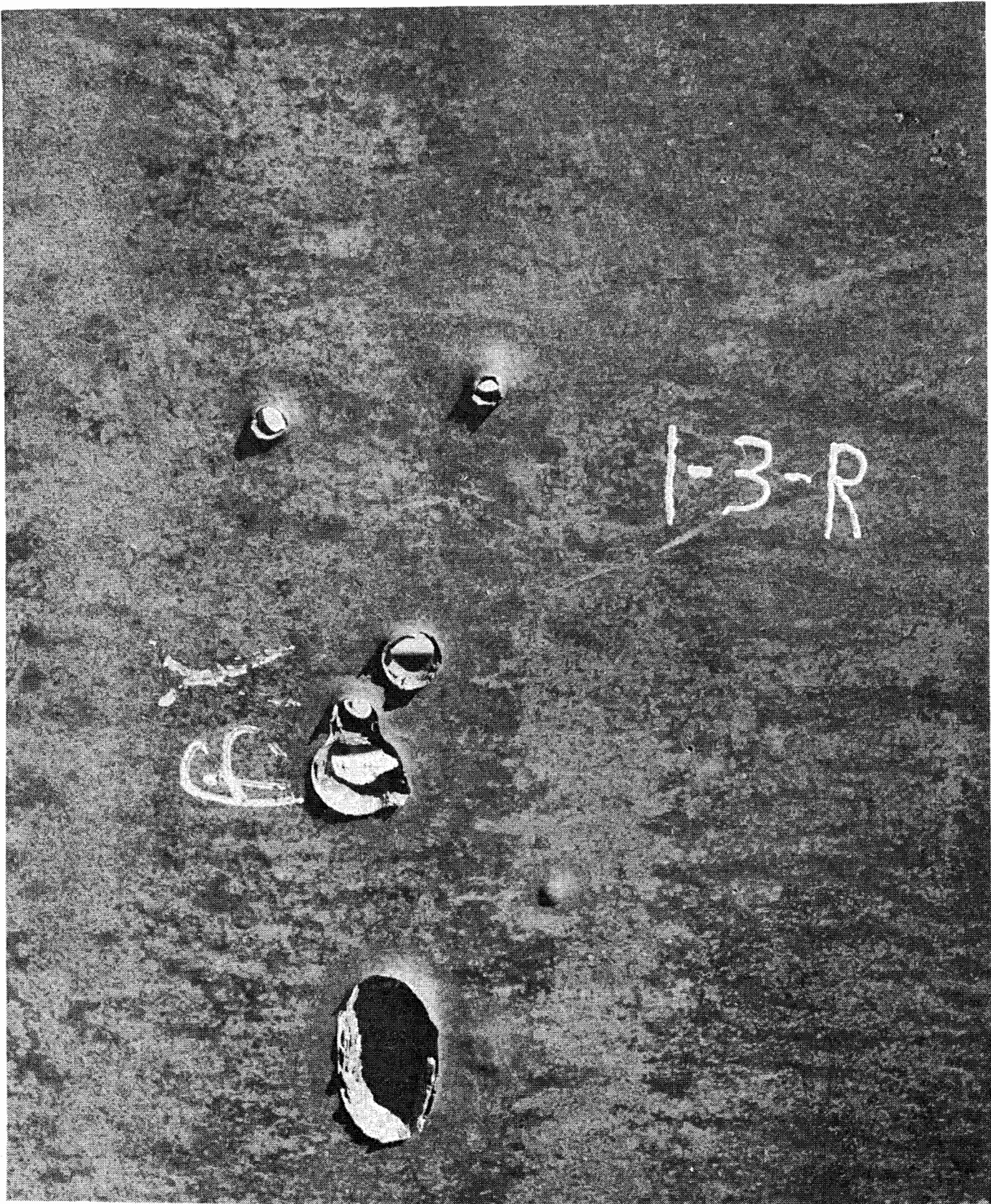


Figure 10. Front View of Third Target Plate After Test



**Figure 11.** Back View of Third Target Plate After Test

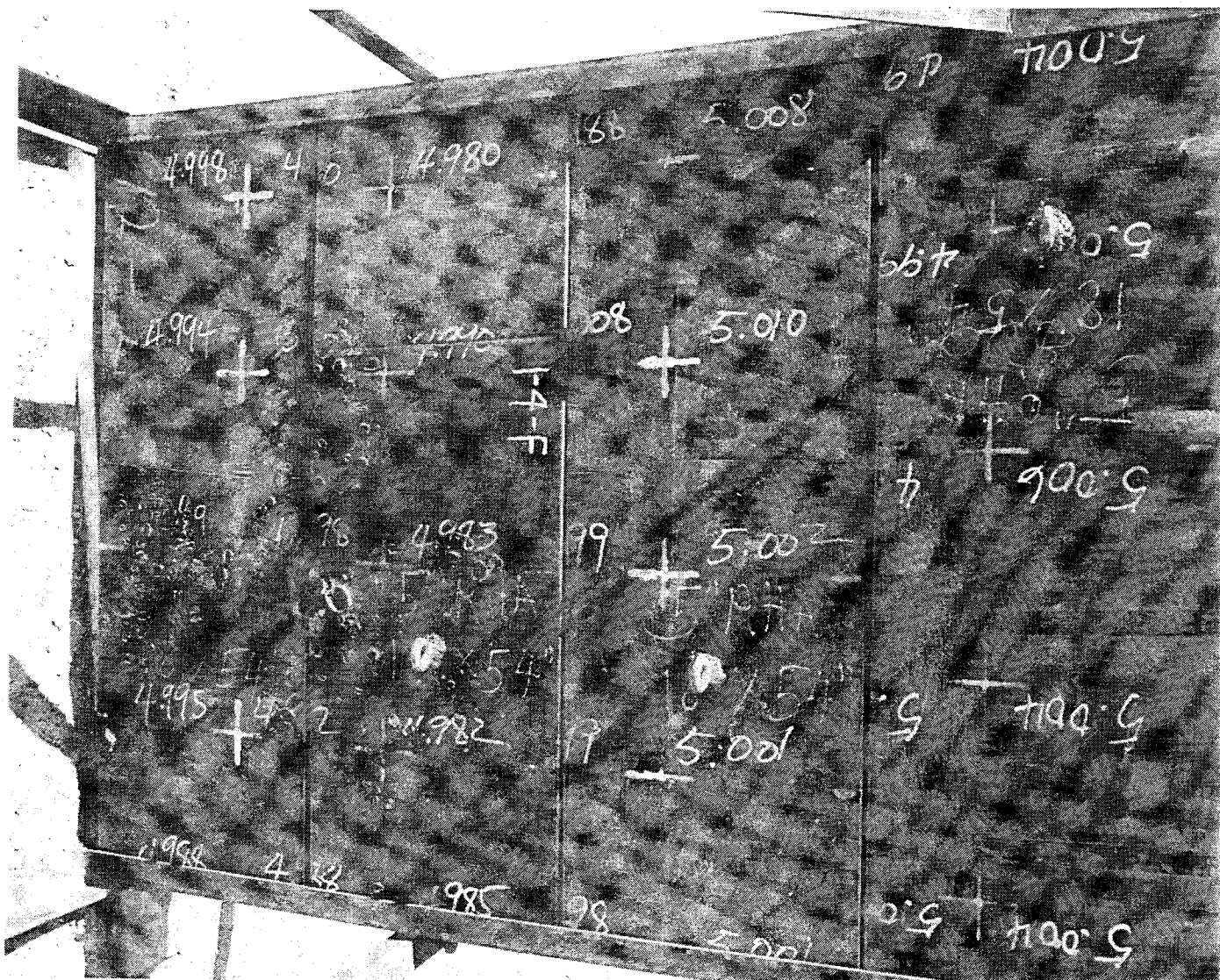


Figure 12. View of Deep Pits Formed in Front of Catcher Plate

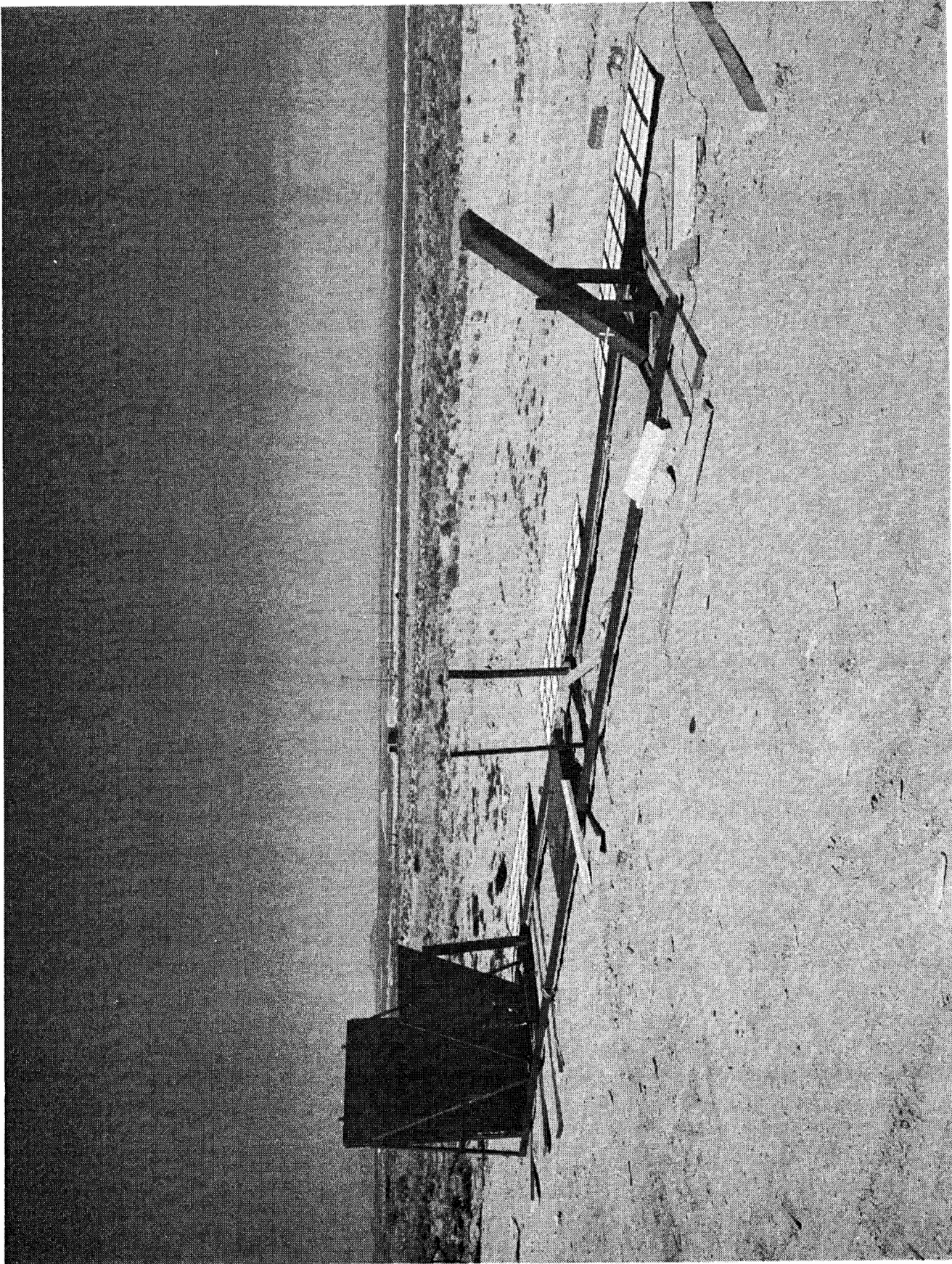


Figure 13. Overall View of Target Array After Test

INTERNAL DISTRIBUTION ONLY:

1520 D. J. McCloskey  
1522 P. P. Stirbis  
1530 L. W. Davison  
1531 S. L. Thompson  
1531 F. J. Zeigler  
1533 P. Yarrington  
1534 J. R. Asay  
1600 R. G. Clem  
1650 D. J. Rigali  
1651 A. K. Miller  
1651 M. W. Sterk  
1652 A. C. Bustamante  
5341 C. E. Dalton  
5341 M. J. Forrestal  
5341 G. E. Reis  
8024 M. A. Pound  
3141 C. M. Ostrander (5)  
3151 W. L. Garner

